Article

Development of Photocatalytic 3D-Printed Cementitious Mortars: Influence of the Curing, Spraying Time Gaps and TiO₂ Coating Rates

Behzad Zahabizadeh [1,†], Iran Rocha Segundo [2,3,†], João Pereira [1,4], Elisabete Freitas [5], Aires Camões [2], Carlos J. Tavares [3], Vasco Teixeira [3], Vítor M. C. F. Cunha [1], Manuel F. M. Costa [6,*] and Joaquim O. Carneiro [3]

1   ISISE, Institute of Science and Innovation for Bio-Sustainability (IB-S), Department of Civil Engineering, University of Minho, 4800-058 Guimarães, Portugal; b.zahabizadeh@civil.uminho.pt or b.zahabizadeh@gmail.com (B.Z.); joaodaniel.pereira@innovpoint.com (J.P.); vcunha@civil.uminho.pt (V.M.C.F.C.)
2   CTAC, Department of Civil Engineering, University of Minho, 4800-058 Guimarães, Portugal; iran_gomes@hotmail.com (I.R.S.); aires@civil.uminho.pt (A.C.)
3   Centre of Physics of Minho and Porto Universities (CF-UM-UP), Azurém Campus, University of Minho, 4800-058 Guimarães, Portugal; ctavares@fisica.uminho.pt (C.J.T.); vasco@fisica.uminho.pt (V.T.); carneiro@fisica.uminho.pt (J.O.C.)
4   Innovation Point, Rua de Pitancinhos—Palmeira, 4700-727 Braga, Portugal
5   ISISE, Department of Civil Engineering, University of Minho, 4800-058 Guimarães, Portugal; efreitas@civil.uminho.pt
6   Centre of Physics of Minho and Porto Universities (CF-UM-UP), Gualtar Campus, University of Minho, 4704-553 Braga, Portugal
*   Correspondence: mfcosta@fisica.uminho.pt
†   These authors contributed equally to this work.

Abstract: This work evaluated the photocatalytic activity of 3D-printed cementitious mortar specimens functionalized with TiO₂ nanoparticles to obtain a multifunctional and smart concrete. This research aims to assess the influence of different parameters related to the functionalization process such as adsorption, coating time gaps, and coating rates on the degradation efficiency of the functionalized cementitious specimens. Each specimen was evaluated under the degradation of Rhodamine B (RhB) in an aqueous solution using a sun-light simulation. The obtained results showed a decrease in adsorption (under dark condition) with increasing the sample curing age. The highest photocatalytic efficiency was observed for coated samples aged 7 days. By increasing the coating rates, the photocatalytic efficiency is enhanced. Nonetheless, regardless of the coating rates, all the specimens showed an increase in photocatalytic efficiency for longer time periods of light exposition, i.e., after 8 h of irradiation.

Keywords: 3D concrete printing; TiO₂ nanoparticles; surface coating; functionalized cementitious materials; smart mortar; photocatalytic mortar

1. Introduction

Air pollutants, in addition to soot fouling, are some agents for both construction's lifespan reduction and deterioration of the buildings' architectural aesthetics [1,2]. Therefore, the need for preventing or reducing environmental pollutants to mitigate their problems and consequences has become an important concern for several industries and research groups [3–5]. The Architecture, Engineering, and Construction (AEC) sector presents a crucial role in this field since structures/buildings/infrastructures, i.e., the built environment, covers a huge area of urban centers. Therefore, the photocatalytic functionalization of construction materials for the built environment has great potential by taking advantage of solar energy in a useful manner by the degradation of different types of pollutants, such

as NO_x and SO_x gases and organic compounds [3,6–9]. Besides the ecological advantages, the aesthetic aspects also have an important role in enhancing the quality of life of human beings since with functionalization it is possible to clean the air [10]. Additionally, the color of the surfaces of buildings and infrastructures that are exposed to the environment changes during their lifetime due to adsorption of pollutants [3,6], which imply additional maintenance work and costs for cleaning their surfaces [8].

Semiconductor photocatalytic materials are able to catalyze the mineralization process of organic and inorganic compounds [3,11]. Titanium dioxide (TiO_2) holds particular features, such as high chemical stability, high oxidation-reduction capacity, non-toxicity, and is available at a lower price, besides being the most employed semiconductor in photocatalytic materials [2,3,8,12–17]. TiO_2 is widely used in different fields for the purpose of water and air purification and self-cleaning [2,18–21], including in civil engineering for cementitious materials (by, e.g., [3–5,7,17,22–25]). The main factors that allow the cementitious materials an ideal support medium for semiconductors (and in particular TiO_2) are: (i) the porous structure of the cementitious mortar/concrete bulk [4,9,24]; (ii) the strong binding ability of the cementitious materials [9,17]; as well as (iii) the compatibility between TiO_2 particles with the alkaline nature of cementitious materials [6,9].

Different methodologies have been used to apply semiconductors into cementitious composites, in order to endow them photocatalytic properties [24]. Volume incorporation during the mixing process (by, e.g., [3,5,22,23]), binder modification [4,15], using the catalytic carrier in the cementitious mixture [24,25], and surface coating by spraying semiconductor particles (by, e.g., [3,5,17,24,26,27]) are some methods used for the photocatalytic functionalization. The coating method by spraying semiconductor particles is recognized as the most efficient and easiest application method for using semiconductors compared to other approaches [17,24]. In the case of adding semiconductors into the mixture composition, it is reported that higher amounts of semiconductors must be used to have the same distribution of TiO_2 particles on the specimens' surface when compared to the surface coating method [5]. On the other hand, using higher amounts of TiO_2 can influence the matrices' rheological (in the fresh state) and mechanical properties [4,5,16,25]. A detailed description of the influence of TiO_2 semiconductors on the properties of cementitious composites can be found elsewhere [16,25].

Regarding the evaluation techniques to assess the photocatalytic efficiency in a broad range of materials (including Civil Engineering Materials—such as asphalt and cementitious), researchers usually carry out methodologies in order to perform the photodegradation of organic compounds (for example, RhB, Methylene Blue, Methylene Orange, among others) (by, e.g., [3,4,9,14,16,22,26,27]). Moreover, multiple factors can affect the photocatalytic behaviour and influence its performance, such as variations in specimens' size, different methodologies for applying pollutants and semiconductor materials and their contents, the light wavelength (UV, visible light, and sun light simulation), and the corresponding power density, the types of dyes and their concentrations, the volume of the dye solution (in the case that dye is used as a pollutant), the time duration of the test, the curing time of the specimens, among others. Therefore, the multiplicity of parameters that have been studied within this topic is one of the main obstacles for the direct comparison between the available results in the literature.

2. Research Significance

In spite of the photocatalytic properties' evaluation of construction materials having started in the early 1990s [16], the research in this field is still ongoing, based on the development of new materials and techniques. For instance, combining photocatalytic technology with new construction methodologies, such as 3D concrete printing (3DCP) may result in the development of functionalized materials through advanced manufacturing techniques. In this case, if a volume incorporation approach is adopted, only the outer layer(s), which are visible, might be functionalized, leading to a more cost-effective material. On the other hand, if the functionalization is carried out by a surface-coating methodology,

this could be employed simultaneously in an automatized way during the printing process, potentiating the photocatalytic efficiency due to the application of TiO$_2$ nanoparticles at an early age of the cementitious composites, which might not be possible in conventionally cast concretes. To the best of the authors' knowledge, the research within the latter field is still scarce [16,23]. Furthermore, the smart and multifunctional cementitious mortar will present photodegradation abilities of adsorbed and air pollutants, and a self-shaping capability, which has practical and cost benefits with prompting construction speed and reducing labour force.

The main scope of this study was to evaluate the potential of adding photocatalytic functionalization with focus on the RhB dye photodegradation efficiency to cementitious materials that have been developed for 3DCP [28]. The 3DCP technology as a freeform construction methodology allows a multitude of advantages; in this context, the specimen surface can be coated right away after finishing the printing process. This possibility can improve the quality of the bonding of the nanoparticles onto the surface of the cementitious specimens when they are still fresh. Therefore, the time gap between the printing process and spraying of the TiO$_2$ nanoparticles could be studied using 3DCP technology, which cannot be applicable to traditional mould cast concrete elements. In the literature, this coating method has also been applied for mould cast concrete specimens. However, for the latter, the semiconductor particles could only be sprayed after removing the moulds, i.e., after an initial hardening of the concrete. In this case, the bond quality between the particles and the specimens' surface could be lower, resulting in the separation of the particles from the surface. This phenomenon was reported under real environmental conditions, in particular due to wind and rain [3,16,29].

In this study, the time gap periods for spraying of TiO$_2$ nanoparticles, the variation of adsorption by curing age, and the influence of coating rates on the photocatalytic efficiency of the 3D-printed cementitious materials were studied. This represents a novelty for the scientific community regarding the photocatalytic properties of coated cementitious concretes, since the spraying of TiO$_2$ nanoparticles can be performed before the hardening of the concrete, on opposition to traditional cast concrete. It is important to emphasize that, as far as the authors are aware, this is one of the first times that nanoparticles of semiconductor materials are applied to functionalize cementitious mortars obtained by a 3D printer (in order to add new functions and/or properties).

3. Photocatalytic Process

The dye degradation promoted by the use of TiO$_2$ nanoparticles in cementitious materials occurs due to two mechanisms related to the photocatalytic activity of TiO$_2$ nanoparticles under light irradiation and through a dye-sensitised approach [22]. This degradation process is based on breaking chemical bonds of the dye chromophore with different bond energies [30]. TiO$_2$ has three electronic band structures, which include the valence band, conduction band and band gap [5,31]. The energy range between the lowest unoccupied state of the conduction band and the highest occupied energy state of the valence band influences the electrical conductivity of a semiconductor material, which will affect the photocatalytic behaviour of such a semiconductor, as is the case of TiO$_2$.

In the first mechanism, the photocatalytic process starts when light photons with a specific wavelength irradiate the semiconductor nanoparticles to activate the electrons of the valence band [14]. If the energy of the absorbed photon (hv) by the semiconductor is equal to or greater than the band gap energy, electrons from the valence band can be promoted to the conduction band, resulting in the separation of electron (e^-) and hole (h^+) charge carriers [14,32,33]:

$$\text{TiO}_2 + hv \ \rightarrow \ h^+ + e^- \tag{1}$$

The h^+ carriers have a powerful oxidation ability and are capable of degrading organic and inorganic compounds into water and other small harmless molecules [5].

The number and lifetime of the generated free (e^-/h^+) pairs depend on the size of the semiconductor particles [14]. For large particles, the volume recombination of

(e^-/h^+) pairs is the dominant process (should be avoided). On the contrary, for small-sized particles, the covered distance by the (e^-/h^+) pairs during their movement from the crystal interface to the particle surface is short; under this condition, the migration rate of the (e^-/h^+) pairs to the surface of small particles is increased, thus minimizing their electronic recombination, which enhances the occurrence of redox reactions and, therefore, improving the photocatalytic efficiency.

In the presence of moisture (water), the highly reactive hydroxyl radicals ($HO^\bullet$) can be formed due to the reaction between h^+ and H_2O [6], see Equation (2). On the other hand, a superoxide ion (O_2^-) can be produced due to the reaction between electron carriers and oxygen [6]; see Equation (3).

$$h^+ + H_2O \rightarrow HO^\bullet + H^+ \tag{2}$$

$$e^- + O_2 \rightarrow O_2^- \tag{3}$$

Both hydroxyl radicals and superoxide ions are highly reactive species that will oxidize the organic/inorganic compounds adsorbed on the semiconductor surface [5]. Moreover, the hydroperoxyl radicals, also known as hydrogen superoxides (HO_2), are created from the reaction between H^+ and O_2^-:

$$H^+ + O_2^- \rightarrow HO_2 \tag{4}$$

Organic compounds can be fully degraded to carbon dioxide (CO_2) and water (H_2O), when they react with hydroxyl radicals [2]:

$$OH + C_nO_mH_{(2n-2m+2)} \rightarrow xCO_2 + yH_2O \tag{5}$$
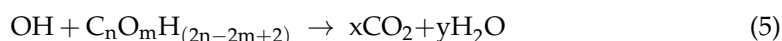
The reaction on Equation (5) can be invoked for different organic materials, such as oil and grease [34] and bio-microorganisms [12]. Figure 1 shows the overall diagram of heterogeneous photocatalysis of organic and inorganic compounds promoted by a semiconductor material.
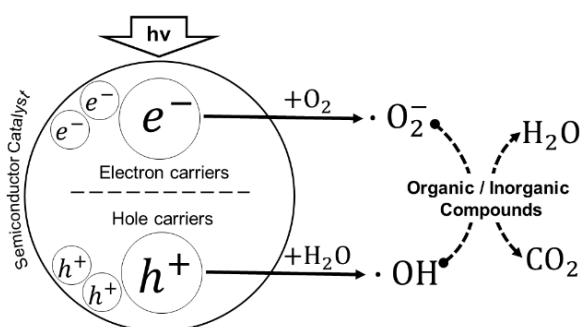
Figure 1. Schematic diagram showing the mechanism of heterogeneous photocatalysis of organic and inorganic compounds promoted by a semiconductor material.

During the second mechanism, the electrons in the highest occupied molecular orbital level (known as HOMO level) of the dye are promoted to the lowest unoccupied molecular orbital level (known as LUMO level) and afterwards inserted within the conductance band of TiO_2 [22]. Then, oxygen uses these electrons to create oxidative species that reduce and subsequently degrade the dye molecules, which are already partially reacted [22,35]. Dye sensitization occurs at lower energies of the visible light that are not sufficiently enough to activate the TiO_2 particles, but can sensitize and degrade the chromophores of the dye.

4. Materials and Experimental Methods

4.1. Materials

The mixture composition was defined in previous experimental works regarding the development and characterization of the mechanical behaviour of ternary cementitious mortars for 3D concrete printing [28,36]. Table 1 includes the constituents used in the selected mortar composition.

**Table 1.** Ternary mortar mixture composition.

Material	Quantity [kg/m^3]	Specific Weight [g/cm^3]
Sand	1183	2.66
Cement (CEM I 42.5 R)	286	3.11
Fly ash (type F)	423	2.35
Silica fume	79	2.25
Water	248	1
Superplasticizer	10.2 [1.3%]	1.04

TiO_2 nanoparticles (nano-TiO_2) were chosen as semiconductor photocatalysts in order to functionalize the 3D-printed cementitious mortar specimens. The TiO_2 nanoparticles (80% anatase and 20% rutile) were purchased from Quimidroga Portugal Lda. (Lisboa, Portugal). Diffuse reflectance as a simple and powerful spectroscopic tool was used to calculate the optical properties of the TiO_2 nanoparticles (namely its band gap energy, Eg). The diffused reflection measurements were acquired from a spectrophotometer ScanSpecUV-vis, ScanSci equipped with an integrating sphere assembly where barium sulphate was used as a reference. The E_g of the photocatalyst was calculated based on Kubelka–Munk theory [37]. Due to the presence of oxygen vacancies, titanium dioxide (TiO_2) is an intrinsically n-type semiconductor material [38] with an energy bandgap equal to 3.2 eV (anatase crystalline phase—indirect allowed transition) and 3.0 eV (rutile crystalline phase—direct allowed transition) [39]. Therefore, the production of an electron in its conduction band and hole in its valence band requires the absorption of a photon with energy in the UV region of the electromagnetic spectrum. In this work, the calculated value for the energy gap of nano-TiO_2 was 3.19 eV, which is an intermediate value for both crystalline phases (anatase and rutile) because it results from a mixture of these two crystalline phases, being slightly lower than the value of the anatase phase.

The nano-TiO_2 aqueous suspensions were prepared based on different concentrations of nanoparticles, namely, 4 g/L, 8 g/L and 16 g/L. A pH of 8 was adopted for all the suspensions. The choice for this pH value was based on its ability to prevent the aggregation of TiO_2 nanoparticles, which results in more stable colloidal suspensions. In fact, at a pH of 8 the zeta potential of the TiO_2 nanoparticles dispersion is negative [8] and, therefore, repulsive electrostatic forces (Coulomb forces) arise that help to promote a better dispersion of the TiO_2 nanoparticles.

4.2. Sample Preparation

The mortar specimens were manufactured through a small 3D concrete printer. The specification and characteristics of the 3D printer can be found elsewhere [28]. In each printing batch, several cementitious mortar strips were printed. Each strip was printed in two layers on top of each other with the dimensions of $250 \times 25 \times 15$ mm^3. The strips were cut right after printing in order to prepare the final specimens with adequate dimensions (i.e., $25 \times 25 \times 15$ mm^3) for the photocatalytic tests (Figure 2a).

| (**a**) | (**b**) |
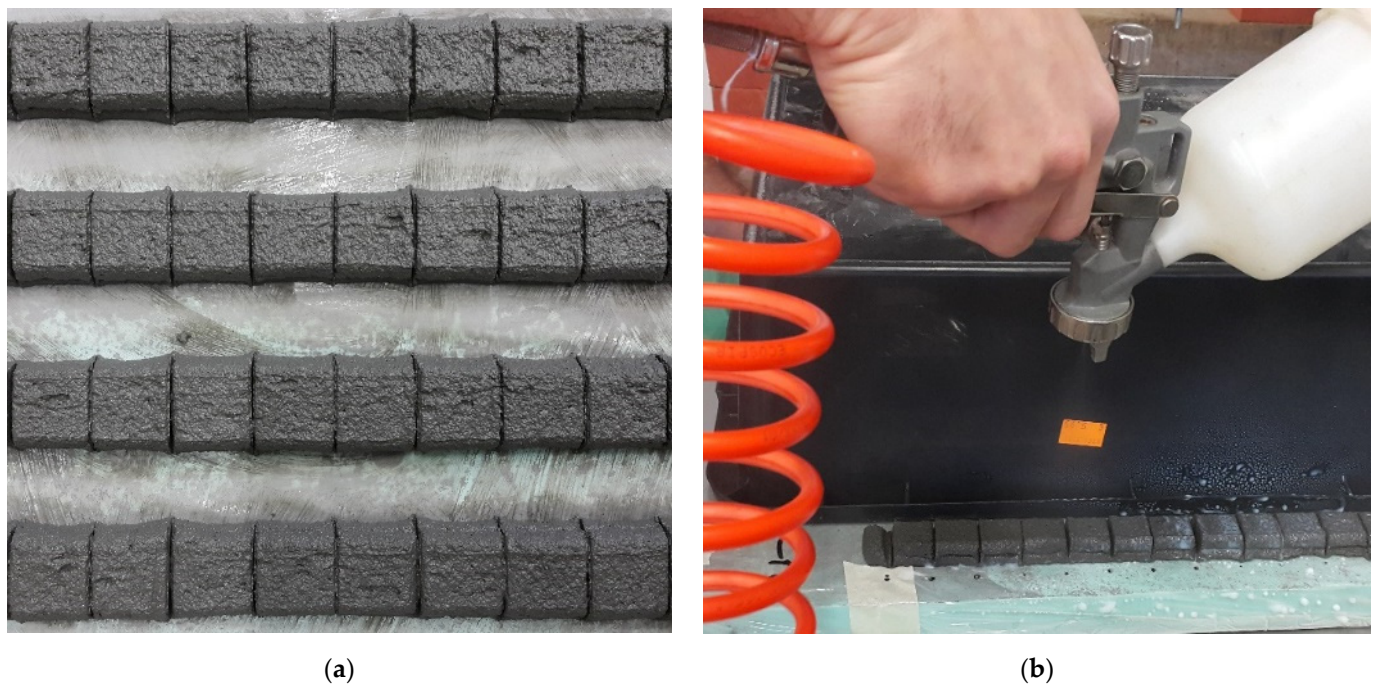
Figure 2. Sample preparation for photocatalytic test: (**a**) the specimens after fresh cutting; (**b**) spraying of TiO$_2$ aqueous suspension using an atmospheric air compressor spray gun.

The spraying coating technique was used as the functionalization method of the samples. The coating was applied by spraying a TiO$_2$ aqueous suspension onto the specimens' surfaces based on our previous work carried out over asphalt mixtures developed by [8,40,41]. This method of functionalizing material surfaces consists of spraying the TiO$_2$ aqueous suspension onto the specimens' surfaces using an atmospheric air compressor (Figure 2b). The distance between the tip of the air compressor and the top surface of the specimens was kept constant at 20 cm, and the spraying was continued for 30 s. Using these parameters, the speed of the aqueous suspension jet was equal to 100 mL/min, which could create coating rates of about 5 mg/cm^2 to 80 mg/cm^2 onto the surface of specimens, based on the known volume of TiO$_2$ aqueous suspensions and the sprayed area. Moreover, in order to evaluate the influence of spraying time gaps on the photocatalytic behaviour of cementitious materials, six different time gaps were chosen to spray the TiO$_2$ aqueous solutions onto the surface of the specimens. The distinct time gaps were selected because the matrices have distinct maturation times, from the time that they are still fresh up to the hardened stage. In this case, the first series of the specimens was coated after 1.5 h of the hydration process initiation. A preliminary test on the cementitious mortar mixture showed an initial setting time of about 5 h. Therefore, the second series was sprayed after 5 h at about the initial of setting time. The other four series were coated at 9, 24, 32 h, and 7 days after the start of hydration process.

4.3. Methodology for Evaluating the Photocatalytic Efficiency

The photocatalytic behaviour of the functionalized cementitious mortar specimens was evaluated based on their capability to promote the photodegradation of a particular organic compound. In this work, RhB dye (a cationic dye, acquired from Merck S.A., Algés, Portugal) has been selected as the pollutant model (due to their wide use in photocatalytic tests) to evaluate the photocatalytic ability of the TiO$_2$ coated-cement mortar specimens. The RhB, which has quite low sensitivity to the alkaline nature of the cementitious materials [4,26], was used in the form of an aqueous solution with concentration of 5 mg/L (5 ppm). The RhB degradation rate in this aqueous solution was measured based on the maximum absorbance of light at a wavelength of 554 nm. All samples were immersed in 30 mL of the RhB solution. After 3 h of immersion under dark conditions, the test

specimens were irradiated by an OSRAM UltraVitalux lamp with 300 W, which simulates the solar irradiation. By keeping a vertical distance of 25 cm between the top surface of the samples and the light source, the specimens were irradiated by light power density equal to 1 mW/cm^2 (measured by a Quantum Photo Radiometer HD9021 Delta Padova). During the irradiation phase, a transparent plastic film covered all the cups containing the RhB solution and the immersed specimens. The plastic film was used to prevent the evaporation of RhB aqueous solution due to the generated heat flux by the lamp. The type of used plastic film could transmit at least 90% of the incident light in the wavelength range between 292 and 900 nm, so it presents a negligible effect on the light wavelength and density received by the test specimens to initiate the photocatalysis.

The test specimens were irradiated for 8 h. After each time period of 1, 2, 4, and 8 h, an aliquot of 3 mL of RhB aqueous solution was extracted from the cup, and its light absorbance was measured in the wavelength ranges of 300 to 800 nm using a Shimadzu UV-310PC scanning spectrophotometer. Afterwards, the photocatalytic efficiency was calculated according to Equation (6) based on the maximum absorbance value at the wavelength of 554 nm using the Beer–Lambert law [8]

$$\Phi \, [\%] = \left(\frac{A_0 - A}{A_0} \right) \times 100 \tag{6}$$

where Φ is the photocatalytic efficiency [%]; A_0 and A are the maximum absorbance of the light by RhB aqueous solution at the time zero and time t, respectively. The time zero was considered as the time of starting the light irradiation at the end of adsorption/desorption equilibrium process.

5. Results and Discussions

5.1. Influence of Curing Age on Adsorption

Figure 3 shows the variation in the specimens' adsorption (reference and functionalized) based on their curing ages, as well the average value (avg) of adsorption for the different series. The results show a reduction of about 74% in the adsorption of the specimens by increasing the curing ages from 2 days to 90 days. However, the reduction rate of the adsorption decreases with the increase in the curing age. The adsorption decreases about 14% from a curing age of 28 days to 90 days. The reduction in the adsorption can be ascribed to the change of the microstructure in cementitious materials during time due to the ongoing hydration process decreasing even their hygroscopic behaviour [7]. During the hydration process, the water inside the pores is substituted by the accumulation of hydration products [11]. Therefore, by increasing the curing time, the decrease in the porosity results in a reduction in the internal absorption and surface adsorption of the specimens. A reduction in the amount of both capillary pores and total volume of pores is reported by [11,42] due to the increase in the curing age in cementitious materials. In a previous study [28] which concerns the mechanical/physical properties of the same cementitious mixture composition of this research, a reduction of about 46% was observed in the porosity of 3D-printed specimens from the curing age of 3 days to 28 days.

The results also reveal that the reduction in the adsorption has occurred for both the reference and the TiO$_2$-coated specimens. Nonetheless, the adsorption of TiO$_2$-coated specimens was higher than the reference ones for each specific curing age. The only exception was observed at the curing age of 14 days, in which the reference specimens showed higher adsorption than the functionalized specimens. The higher adsorption of functionalized specimens may be attributed to the presence of the TiO$_2$ nanoparticles on the specimen surfaces. The high specific surface area of the TiO$_2$ nanoparticles on the coated specimens could enhance the adsorption through the negatively charged surface of TiO$_2$ particles [43] when compared to the reference specimens without any kind of coating. For longer curing times (i.e., 28 and 90 days) the reduction in the dye concentration is mainly due to the decomposition of dye adsorbed on the surface of the specimen through the photocatalytic activity of semiconductors. However, at early ages, a higher amount

of dye is absorbed by the porous structure of the material due to the existence of larger pores and a higher amount of pore volume. Therefore, it is more difficult to distinguish between the real photocatalytic behaviour of the material due to semiconductor inherent photocatalytic activity and the dye degradation due to internal absorption. Moreover, larger pores present mainly during the early curing ages may absorb the dye molecules into the matrix in deeper zones that neither the semiconductor particles (in the coating approach) nor the light can reach, which was reported as an adverse effect of the large pores against the photocatalytic efficiency [9]. The results in tabular format can be found in the supplementary material as Table S1.
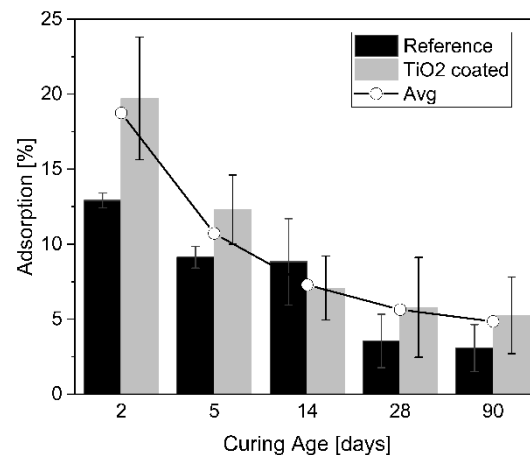
**Figure 3.** Variation of adsorption by curing age for reference and TiO$_2$ coated specimens.

5.2. Influence of the Spraying Time Gap on the Photocatalytic Efficiency

The influence of the spraying time gap on the photocatalytic behaviour was assessed for the same coating rate of 5 mg/cm^2. The coating time gap was defined based on the initiation of the hydration process, namely, since the initial instant when water was added to the mixture composition. The distinct spraying time gaps were defined in order to have different surface conditions of the 3D-printed specimens, from the early ages, in which the mixture is completely fresh, up to when it is hardened (See Section 4.2). The specimens coated at distinct time gaps of 1.5, 5, 9, 24, 32 hours and 7 days were named as SP_1.5 h, SP_5 h, SP_9 h, SP_24 h, SP_32 h, and SP_7 d, respectively. The photocatalytic test was carried out for all the specimens after 28 days of curing process.

Figure 4 shows the photocatalytic efficiency of the specimens based on the distinct spraying time gaps. All the specimens showed an enhancement of the photocatalytic efficiency from the beginning of light irradiation. During the entire time of the testing procedure, the specimens coated at the age of 7 days showed the highest photocatalytic efficiency when compared to the specimens coated with fewer days of curing. At the end of the testing procedure, after 8 h of light irradiation, the series SP_9 h showed the lowest photocatalytic efficiency of about 19%, which translates to a difference of about 47% between the maximum (i.e., SP_7 d) and the minimum (i.e., SP_9 h) photocatalytic efficiencies.

Regardless of the specimen SP_7 d, the results obtained by the other specimens revealed similar photocatalytic behaviour. In this case, the maximum difference between the efficiencies of specimens coated at the ages of 32 (SP_32 h) and 9 h (SP_9 h) was about 15%. On the other hand, the photocatalytic efficiency of specimens SP_32 h was just 4% higher than the efficiency of specimens coated at the age of 1.5 h (SP_1.5 h), which could be considered negligible.
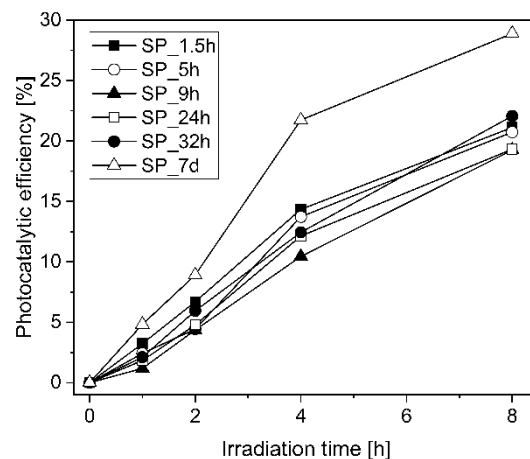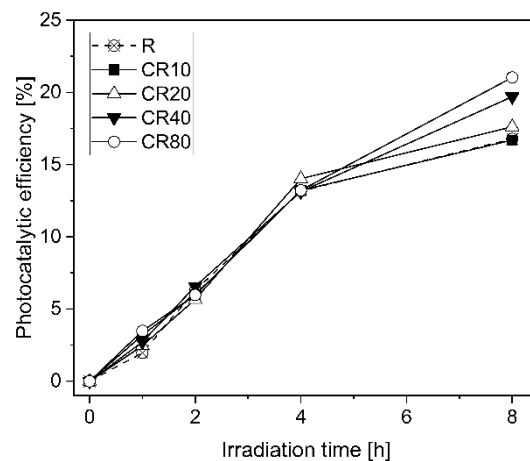
Figure 4. The influence of the TiO$_2$ coating time gap on the photocatalytic efficiency.

The similarity of the results reveals that the difference in coating time does not extensively influence the photocatalytic efficiency. However, the better behaviour observed by specimen SP_7 d shows the need for further research for larger time gaps. Nonetheless, the coating at the beginning of the hydration process, when the mixture is still fresh, can improve the immobilization of TiO$_2$ nanoparticles to the surface of mortar specimens. Moreover, the alkaline nature of the cementitious matrices can properly create a suitable substrate for the immobilization of the TiO$_2$ nanoparticles [6]. Nevertheless, these aspects need to be evaluated. As the 3D-printing technology is a free-form construction process [28], it is feasible to spray the TiO$_2$ aqueous suspension immediately after printing the elements in order to improve the bonding properties. On the other hand, the results obtained for the specimens coated at the age of 7 days could also demonstrate the efficiency of this type of functionalizing method for hardened cementitious specimens. The spraying of TiO$_2$ aqueous suspension after drying the cementitious material was also tried [3]. However, a poor dye degradation behaviour was reported, which results from the partial separation of the semiconductors' surface layer due to exposure to environmental conditions such as wind and rain [3]. The results in tabular format can be found in the supplementary material as Table S2.

5.3. Influence of the TiO$_2$ Coating Rates on the Photocataytic Efficiency

Figure 5 shows the photocatalytic efficiency of functionalized specimens with different TiO$_2$ coating rates of 10, 20, 40 and 80 mg/cm^2 (designated as CR10, CR20, CR40 and CR80, respectively). An increase in the photocatalytic efficiency was observed from the beginning of the light irradiation procedure for all the TiO$_2$-coated specimens regardless of their coating rates. Moreover, the reference specimen without surface coating also showed an increase in degradation efficiency up to the end of 8 h of light irradiation.

When comparing all the series, a similar photocatalytic behaviour by all the TiO$_2$-coated and reference specimens was observed up to 4 h of irradiation. Increasing the time period of light irradiation up to 8 h produced more significant differences in the photocatalytic efficiency of the different series. After 8 h of light irradiation, the highest efficiency of about 21% is ascribed to CR80. The lowest photocatalytic efficiency was observed for CR10 and the reference series, both around 17%. Therefore, for a larger irradiation period of 8 h, a difference of about 26% was observed between the maximum and the minimum photocatalytic efficiencies of the specimens. Moreover, regarding the coating rates, an increase in the photocatalytic efficiency by increasing the coating rates of TiO$_2$ nanoparticles was observed. The increase in photocatalytic efficiency by increasing the coating rates was also reported by [8] for the TiO$_2$ surface coated asphalt samples.

Figure 5. The influence of TiO$_2$ coating rates on the photocatalytic efficiency.

The lack of enough TiO$_2$ nanoparticles coverage on the surface of the specimens of these series can be pointed out as a hypothesis for the similarity between the photocatalytic behaviour of the reference and the CR10 series. Nonetheless, further assessment is necessary to find the main reason for this behaviour.

The similar photocatalytic efficiency for all the series up to 4 h of light irradiation may be ascribed to the accumulation of adsorbed pollutants and the produced dye decomposition products onto the specimens' surface, which could partially inactivate the reaction sites [44]. Nonetheless, by increasing the light exposure period up to 8 h, the reaction products generated by the degradation mechanism had enough time to be removed from the surface of the specimen, and the TiO$_2$ nanoparticles could be reactivated in order to degrade a higher quantity of pollutants. Clearer differences between the photocatalytic efficiencies after 8 h of irradiation can be a confirmation for the observed behaviour. The results in tabular format can be found in the supplementary material as Table S3.

6. Conclusions

In this study, the photocatalytic behaviour of 3D-printed cementitious mortar specimens coated with TiO$_2$ nanoparticles was evaluated under their photocatalytic efficiency. Different parameters, such as adsorption against curing age, coating time gap (based on the initiation of the matrix hydration), and coating rates were evaluated regarding their influence on photocatalytic behaviour. The obtained results can be summarized as follows:

- Adsorption in cementitious materials decreases with increasing curing age. This can be ascribed to the change in the matrix microstructure while the hydration process is ongoing. However, the adsorption of the functionalized specimens coated with TiO$_2$ nanoparticles was higher when compared to the reference specimens, regardless of the curing ages that have been analysed. The high specific surface area of TiO$_2$ nanoparticles could be the main reason for higher adsorption on the functionalized specimens.

- The coating time measured from the beginning of hydration process did not have a significant influence on the photocatalytic efficiency. The only exception occurred for the specimens SP_7d, i.e., coated for 7 days, which showed 47% higher photocatalytic efficiency when compared to the other specimens. Nonetheless, the coating at the beginning of the hydration process when the mixture is still fresh can improve the bonding of TiO$_2$ particles to the surface of the cementitious mortar specimens. Therefore, using the advantages of the 3D printing technology as a free-form construction methodology, the TiO$_2$ aqueous suspension can be sprayed immediately after printing the elements. On the other hand, adequate results obtained for the specimens coated and aged for 7 days could also demonstrate the efficiency of this type of functionalizing method for hardened cementitious matrices. However, TiO$_2$ particles sprayed onto the dried cementitious surfaces may be more prone to be separated from the spec-

imens, which may lead to a decrease in photocatalytic efficiency of samples exposed to real environmental conditions.

- The photocatalytic efficiency could be enhanced by increasing the coating rates of the TiO_2 nanoparticles onto the surface of the specimens. After 8 h of light irradiation, photocatalytic efficiencies of 17% and 21% were obtained for the lowest and the highest coating rates of 10 and 80 mg/cm^2, respectively. Similar photocatalytic behaviour for all the series up to 4 h of irradiation was observed. This behaviour may be ascribed to the accumulation of adsorbed pollutants and the produced dye decomposition products onto the specimens' surface, which could partially inactivate the reaction sites. Nonetheless, by increasing the light exposure period up to 8 h, the reaction products created from the degradation mechanism have enough time to be removed from the surface of the specimen and the TiO_2 nanoparticles could be reactivated again in order to degrade a higher quantity of pollutants.

The combination of two techniques, namely the application of TiO_2 and 3D printing, is an innovative topic of smart materials by the development of two new capabilities to mortars, which are photocatalytic and also 3D printable. These functionalized surfaces could photodegrade gases, such as SO_x and NO_x, and adsorb organic compounds, cleaning the air and maintaining the aesthetic aspects of buildings and infrastructures.

References

1. Smits, M.; Chan, C.K.; Tytgat, T.; Craeye, B.; Costarramone, N.; Lacombe, S.; Lenaerts, S. Photocatalytic Degradation of Soot Deposition: Self-Cleaning Effect on Titanium Dioxide Coated Cementitious Materials. *Chem. Eng. J.* **2013**, *222*, 411–418. [CrossRef]
2. Rocha Segundo, I.; Freitas, E.; Landi, S., Jr.; Costa, M.F.M.; Carneiro, J.O. Smart, Photocatalytic and Self-Cleaning Asphalt Mixtures: A Literature Review. *Coatings* **2019**, *9*, 696. [CrossRef]
3. Diamanti, M.V.; Ormellese, M.; Pedeferri, M. Characterization of Photocatalytic and Superhydrophilic Properties of Mortars Containing Titanium Dioxide. *Cem. Concr. Res.* **2008**, *38*, 1349–1353. [CrossRef]
4. Sikora, P.; Cendrowski, K.; Markowska-Szczupak, A.; Horszczaruk, E.; Mijowska, E. The Effects of Silica/Titania Nanocomposite on the Mechanical and Bactericidal Properties of Cement Mortars. *Constr. Build. Mater.* **2017**, *150*, 738–746. [CrossRef]
5. Chen, C.; Tang, B.; Cao, X.; Gu, F.; Huang, W. Enhanced Photocatalytic Decomposition of NO on Portland Cement Concrete Pavement Using Nano-TiO_2 Suspension. *Constr. Build. Mater.* **2021**, *275*, 122135. [CrossRef]
6. Cassar, L. Photocatalysis of Cementitious Materials: Clean Buildings and Clean Air. *MRS Bull.* **2004**, *29*, 328–331. [CrossRef]

7. Chen, J.; Poon, C.-S. Photocatalytic Activity of Titanium Dioxide Modified Concrete Materials—Influence of Utilizing Recycled Glass Cullets as Aggregates. *J. Environ. Manag.* **2009**, *90*, 3436–3442. [CrossRef]

8. Carneiro, J.O.; Azevedo, S.; Teixeira, V.; Fernandes, F.; Freitas, E.; Silva, H.; Oliveira, J. Development of Photocatalytic Asphalt Mixtures by the Deposition and Volumetric Incorporation of TiO$_2$ Nanoparticles. *Constr. Build. Mater.* **2013**, *38*, 594–601. [CrossRef]

9. Jimenez-Relinque, E.; Rodriguez-Garcia, J.R.; Castillo, A.; Castellote, M. Characteristics and Efficiency of Photocatalytic Cementitious Materials: Type of Binder, Roughness and Microstructure. *Cem. Concr. Res.* **2015**, *71*, 124–131. [CrossRef]

10. Ramirez, A.M.; De Belie, N. Application of TiO$_2$ Photocatalysis to Cementitious Materials for Self-Cleaning Purposes. In *Applications of Titanium Dioxide Photocatalysis to Construction Materials*; Ohama, Y., Van Gemert, D., Eds.; Springer: Dordrecht, The Netherlands, 2011; ISBN 978-94-007-1296-6.

11. Essawy, A.A.; El. Aleem, S.A. Physico-Mechanical Properties, Potent Adsorptive and Photocatalytic Efficacies of Sulfate Resisting Cement Blends Containing Micro Silica and Nano-TiO$_2$. *Constr. Build. Mater.* **2014**, *52*, 1–8. [CrossRef]

12. Banerjee, S.; Gopal, J.; Muraleedharan, P.; Tyagi, A.; Raj, B. Physics and Chemistry of Photocatalytic Titanium Dioxide: Visualization of Bactericidal Activity Using Atomic Force Microscopy. *Curr. Sci.* **2006**, *90*, 1378–1383.

13. Aïssa, A.H.; Puzenat, E.; Plassais, A.; Herrmann, J.-M.; Haehnel, C.; Guillard, C. Characterization and Photocatalytic Performance in Air of Cementitious Materials Containing TiO$_2$. Case Study of Formaldehyde Removal. *Appl. Catal. B Environ.* **2011**, *107*, 1–8. [CrossRef]

14. Carneiro, J.O.; Teixeira, V.; Portinha, A.; Dupák, L.; Magalhães, A.; Coutinho, P. Study of the Deposition Parameters and Fe-Dopant Effect in the Photocatalytic Activity of TiO$_2$ Films Prepared by Dc Reactive Magnetron Sputtering. *Vacuum* **2005**, *78*, 37–46. [CrossRef]

15. Kamaruddin, S.; Stephan, D. Sol–Gel Mediated Coating and Characterization of Photocatalytic Sand and Fumed Silica for Environmental Remediation. *Water. Air. Soil Pollut.* **2014**, *225*, 1948. [CrossRef]

16. Hamidi, F.; Aslani, F. TiO$_2$-Based Photocatalytic Cementitious Composites: Materials, Properties, Influential Parameters, and Assessment Techniques. *Nanomaterials* **2019**, *9*, 1444. [CrossRef] [PubMed]

17. Feng, S.; Song, J.; Liu, F.; Fu, X.; Guo, H.; Zhu, J.; Zeng, Q.; Peng, X.; Wang, X.; Ouyang, Y.; et al. Photocatalytic Properties, Mechanical Strength and Durability of TiO$_2$/Cement Composites Prepared by a Spraying Method for Removal of Organic Pollutants. *Chemosphere* **2020**, *254*, 126813. [CrossRef] [PubMed]

18. Fernandez, F.; Germinario, S.; Basile, R.; Montagno, R.; Kapetanaki, K.; Gobakis, K.; Kolokotsa, D.; Lagou, A.M.; Dania, P.; Enna, M.T.; et al. Development of Eco-Friendly and Self-Cleaning Lime-Pozzolan Plasters for Bio-Construction and Cultural Heritage. *Buildings* **2020**, *10*, 172. [CrossRef]

19. Ao, C.H.; Lee, S.C. Indoor Air Purification by Photocatalyst TiO$_2$ Immobilized on an Activated Carbon Filter Installed in an Air Cleaner. *Chem. Eng. Sci.* **2005**, *60*, 103–109. [CrossRef]

20. Anderson, A.-L.; Chen, S.; Romero, L.; Top, I.; Binions, R. Thin Films for Advanced Glazing Applications. *Buildings* **2016**, *6*, 37. [CrossRef]

21. Hakki, A.; Yang, L.; Wang, F.; Elhoweris, A.; Alhorr, Y.; Macphee, D. Photocatalytic Functionalized Aggregate: Enhanced Concrete Performance in Environmental Remediation. *Buildings* **2019**, *9*, 28. [CrossRef]

22. Folli, A.; Pade, C.; Hansen, T.B.; De Marco, T.; Macphee, D.E. TiO$_2$ Photocatalysis in Cementitious Systems: Insights into Self-Cleaning and Depollution Chemistry. *Cem. Concr. Res.* **2012**, *42*, 539–548. [CrossRef]

23. Bao, Y.; Xu, M.; Soltan, D.; Xia, T.; Shih, A.; Clack, H.L.; Li, V.C. Three-Dimensional Printing Multifunctional Engineered Cementitious Composites (ECC) for Structural Elements. In *First RILEM International Conference on Concrete and Digital Fabrication—Digital Concrete 2018*; Wangler, T., Flatt, R.J., Eds.; Springer International Publishing: Cham, Switzerland, 2019; Volume 19, pp. 115–128. ISBN 978-3-319-99518-2.

24. Han, B.; Zhang, L.; Ou, J. *Smart and Multifunctional Concrete toward Sustainable Infrastructures*; Springer: Singapore, 2017; ISBN 978-981-10-4348-2.

25. Han, B.; Ding, S.; Wang, J.; Ou, J. *Nano-Engineered Cementitious Composites: Principles and Practices*; Springer: Singapore, 2019; ISBN 9789811370779.

26. Ruot, B.; Plassais, A.; Olive, F.; Guillot, L.; Bonafous, L. TiO$_2$-Containing Cement Pastes and Mortars: Measurements of the Photocatalytic Efficiency Using a Rhodamine B-Based Colourimetric Test. *Sol. Energy* **2009**, *83*, 1794–1801. [CrossRef]

27. Campos Teixeira, A.H.; Soares Junior, P.R.R.; Silva, T.H.; Barreto, R.R.; da Silva Bezerra, A.C. Low-Carbon Concrete Based on Binary Biomass Ash—Silica Fume Binder to Produce Eco-Friendly Paving Blocks. *Materials* **2020**, *13*, 1534. [CrossRef]

28. Zahabizadeh, B.; Pereira, J.; Gonçalves, C.; Pereira, E.N.B.; Cunha, V.M.C.F. Influence of the Printing Direction and Age on the Mechanical Properties of 3D Printed Concrete. *Mater. Struct.* **2021**, *54*, 73. [CrossRef]

29. Chen, J.; Poon, C. Photocatalytic Construction and Building Materials: From Fundamentals to Applications. *Build. Environ.* **2009**, *44*, 1899–1906. [CrossRef]

30. Liu, T.; Wang, L.; Lu, X.; Fan, J.; Cai, X.; Gao, B.; Miao, R.; Wang, J.; Lv, Y. Comparative Study of the Photocatalytic Performance for the Degradation of Different Dyes by ZnIn$_2$S$_4$: Adsorption, Active Species, and Pathways. *RSC Adv.* **2017**, *7*, 12292–12300. [CrossRef]

31. Kang, X.; Liu, S.; Dai, Z.; He, Y.; Song, X.; Tan, Z. Titanium Dioxide: From Engineering to Applications. *Catalysts* **2019**, *9*, 191. [CrossRef]

32. Fujishima, A.; Zhang, X.; Tryk, D. TiO$_2$ Photocatalysis and Related Surface Phenomena. *Surf. Sci. Rep.* **2008**, *63*, 515–582. [CrossRef]

33. Wang, Q.; Zheng, K.; Yu, H.; Zhao, L.; Zhu, X.; Zhang, J. Laboratory Experiment on the Nano-TiO$_2$ Photocatalytic Degradation Effect of Road Surface Oil Pollution. *Nanotechnol. Rev.* **2020**, *9*, 922–933. [CrossRef]

34. Bogutyn, S.; Arboleda, C.; Bordelon, A.; Tikalsky, P. Rejuvenation Techniques for Mortar Containing Photocatalytic TiO$_2$ Material. *Constr. Build. Mater.* **2015**, *96*, 96–101. [CrossRef]

35. Ajmal, A.; Majeed, I.; Malik, R.N.; Idriss, H.; Nadeem, M.A. Principles and Mechanisms of Photocatalytic Dye Degradation on TiO$_2$ Based Photocatalysts: A Comparative Overview. *RSC Adv.* **2014**, *4*, 37003–37026. [CrossRef]

36. Zahabizadeh, B.; Pereira, J.; Gonçalves, C.; Cunha, V.M.C.F. Development of Cement-Based Mortars for 3D Printing through Wet Extrusion. In Proceedings of the IABSE Symposium 2019 Guimarães: Towards a Resilient Built Environment—Risk and Asset Management, Guimarães, Portugal, 27–29 March 2019.

37. Carneiro, J.O.; Azevedo, S.; Fernandes, F.; Freitas, E.; Pereira, M.; Tavares, C.J.; Lanceros-Méndez, S.; Teixeira, V. Synthesis of Iron-Doped TiO$_2$ Nanoparticles by Ball-Milling Process: The Influence of Process Parameters on the Structural, Optical, Magnetic, and Photocatalytic Properties. *J. Mater. Sci.* **2014**, *49*, 7476–7488. [CrossRef]

38. Hernández-Alonso, M.D.; Fresno, F.; Suárez, S.; Coronado, J.M. Development of Alternative Photocatalysts to TiO$_2$: Challenges and Opportunities. *Energy Environ. Sci.* **2009**, *2*, 1231. [CrossRef]

39. Khan, A.F.; Mehmood, M.; Durrani, S.K.; Ali, M.L.; Rahim, N.A. Structural and Optoelectronic Properties of Nanostructured TiO$_2$ Thin Films with Annealing. *Mater. Sci. Semicond. Process.* **2015**, *29*, 161–169. [CrossRef]

40. Rocha Segundo, I.; Landi, S., Jr.; Oliveira, S.M.B.; Freitas, E.F.; Carneiro, J.A.O. Photocatalytic Asphalt Mixtures: Mechanical Performance and Impacts of Traffic and Weathering Abrasion on Photocatalytic Efficiency. *Catal. Today* **2019**, *326*, 94–100. [CrossRef]

41. Rocha Segundo, I.; Landi, S., Jr.; Oliveira, S.; Freitas, E.; Costa, M.F.; Carneiro, J. Photocatalytic Asphalt Mixtures: Semiconductors' Impact in Skid Resistance and Texture. *Road Mater. Pavement Des.* **2019**, *20*, S578–S589. [CrossRef]

42. Espinosa, R.M.; Franke, L. Influence of the Age and Drying Process on Pore Structure and Sorption Isotherms of Hardened Cement Paste. *Cem. Concr. Res.* **2006**, *36*, 1969–1984. [CrossRef]

43. Folli, A.; Jakobsen, U.H.; Guerrini, G.L.; Macphee, D.E. Rhodamine B Discolouration on TiO$_2$ in the Cement Environment: A Look at Fundamental Aspects of the Self-Cleaning Effect in Concretes. *J. Adv. Oxid. Technol.* **2009**, *12*, 126–133. [CrossRef]

44. Enesca, A.; Isac, L. The Influence of Light Irradiation on the Photocatalytic Degradation of Organic Pollutants. *Materials* **2020**, *13*, 2494. [CrossRef]